

Development of 7-membered N-heterocyclic carbene ligands for transition metals

Christopher C. Scarborough, Brian V. Popp, Ilia A. Guzei, Shannon S. Stahl *

Department of Chemistry, University of Wisconsin-Madison, 1101 University Avenue, Madison, WI 53706, United States

Received 1 June 2005; received in revised form 12 August 2005; accepted 12 August 2005

Available online 22 September 2005

Abstract

We recently reported the first example of a seven-membered N-heterocyclic carbene (NHC) ligand for transition metals. These ligands are attractive because the heterocyclic framework, derived from 2,2'-diaminobiphenyl, exhibits a torsional twist that results in a chiral, C_2 -symmetric structure. The present report outlines the synthetic efforts that led to the development of these ligands together with the synthesis and structural characterization of metal complexes bearing seven-membered NHCs as ancillary ligands. The identity of nitrogen substituent, neopentyl versus 2-adamantyl, influences the synthetic accessibility and stability of the seven-membered amidinium salts and the NHC–metal complexes obtained via in situ deprotonation/metallation. Computational analysis of the seven-membered ring structures reveals the Hückel antiaromatic 8π electron system achieves significant Möbius aromatic stabilization upon undergoing torsional distortion of the heterocyclic ring.

© 2005 Elsevier B.V. All rights reserved.

Keywords: N-heterocyclic carbene; Palladium; X-ray structure

1. Introduction

N-heterocyclic carbenes (NHCs) continue to emerge as a powerful class of ligands for transition metals [1–3]. Although most NHCs are derived from 5-membered heterocycles [4] (2–4, Fig. 1), 4- and 6-membered analogs have also been reported recently (1, 5 and 6, Fig. 1) [5,6]. In addition, transition metal complexes possessing acyclic carbene ligands have been described [7]. NHC ligands are attractive because they exhibit electronic properties similar to phosphines but tend to be less substitutionally labile [2,8] and have greater stability under oxidative conditions [2b,9,10]. Despite these advantages, successful applications of NHCs in asymmetric catalysis still lag significantly behind phosphines, and the development of new chiral NHC ligands is an area of active interest [2c]. A key limitation of most known NHCs is the presence of a planar or nearly planar heterocyclic framework, which constrains

the spatial orientation of the substituents. Some success has been achieved with chiral chelating NHC ligands [2c], but the identification of new frameworks for the preparation of chiral NHCs could have important implications for asymmetric catalysis. With this goal in mind, we have prepared transition metal complexes possessing the first examples of seven-membered NHC ligands (7, Fig. 1) derived from 2,2'-diaminobiphenyl (8^H) [11,12]. These ligands exhibit a torsional twist that results in an axially chiral structure. Herein, we outline the synthetic efforts that led to the development of this new class of NHC ligands, together with solid state structures of a silver(I) and several palladium(II) complexes bearing these ligands.

2. Results and discussion

2.1. Attempted synthesis of seven-membered-ring amidinium salts with N-aryl substituents

Sterically encumbered aryl groups such as 2,6-diisopropylphenyl and 2,4,6-trimethylphenyl (mesityl), are among

* Corresponding author. Tel.: +1 608 265 6288; fax: +1 608 262 6143.
E-mail address: stahl@chem.wisc.edu (S.S. Stahl).

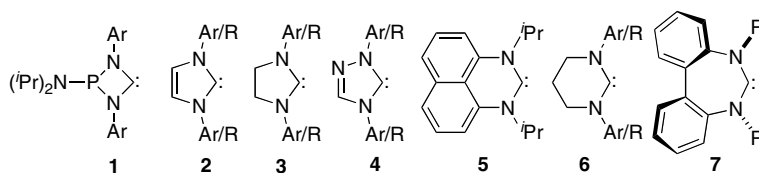


Fig. 1. NHC frameworks currently in the literature.

the most common substituents that have been used in the preparation of stable NHCs and NHC–metal complexes. We therefore targeted variants of **7** bearing *N*-mesityl groups (Fig. 2). Mesylation of **8^H** was very successful under previously reported conditions [13], yielding the dimesylation product **8^{Mes}** in 99% yield. Attempts to install the carbene carbon by using a number of previously reported protocols [14], however, were unsuccessful. This lack of success may reflect the weak nucleophilicity of the diaryl-substituted nitrogen atoms, and therefore, we shifted our attention to *N*-alkylated variants of **8^H**, for which the nitrogen centers should be more nucleophilic.

2.2. Synthesis of seven-membered-ring amidinium salts with *N*-alkyl substituents

N-alkylated NHC-HBF₄ species were easily accessed via cyclization of *N,N'*-dialkyl diamines in the presence of orthoesters under acidic conditions. Neopentyl (Np) groups were installed by adding pivaloyl chloride to **8^H** followed by reduction with lithium aluminum hydride (LAH) [15], and the diamine **8^{Np}** was obtained in 91% overall yield. Complex **8^{Np}** was heated in neat triethyl orthoformate in the presence of NH₄BF₄ [14] to produce pure NHC-HBF₄ **9^{Np}** in 93% yield without need for further purification (Fig. 3). The structure of **9^{Np}** was unambiguously assigned by single-crystal X-ray diffraction analysis [16] (Fig. 4).

Amidinium salts are common precursors to stable NHCs [1,2]; however, the free carbene, **7^{Np}**, was not accessible by

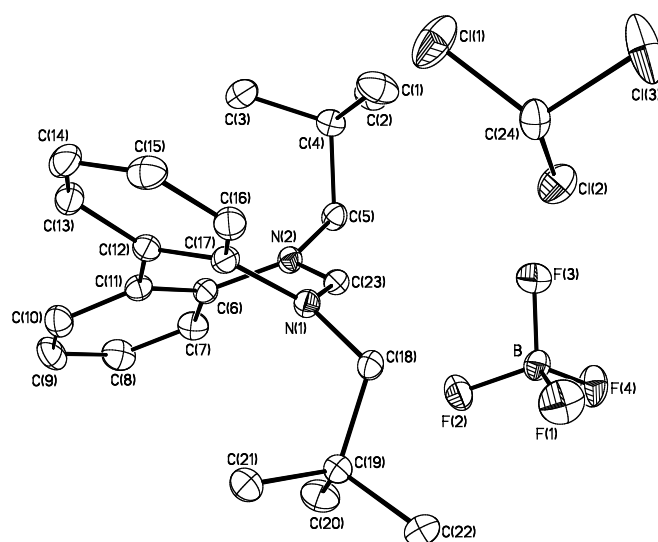


Fig. 4. Solid-state molecular structure of **9^{Np}**, showing BF₄[−] counterion and solvent molecule. Hydrogen atoms are omitted for clarity. Thermal ellipsoids are shown at 50% probability. Selected bond lengths (Å) and angles (°): C23–N1 1.3252(19), C23–N2 1.3154(19), N1–C17 1.4515(18), N2–C6 1.4523(19), C17–C12 1.398(2), C6–C11 1.395(2), C11–C12 1.483(2); N1–C23–N2 127.07(13), C23–N1–C18 115.52(12), C23–N2–C5 116.27(12), C6–C11–C12–C17 40.6(2).

simple deprotonation of rigorously dried **9^{Np}** with carbonate, hydride (with and without catalytic alkoxide), alkoxide, amide, or carbanion bases. Decomposed starting material was obtained in all cases. In all but one case, the amidinium

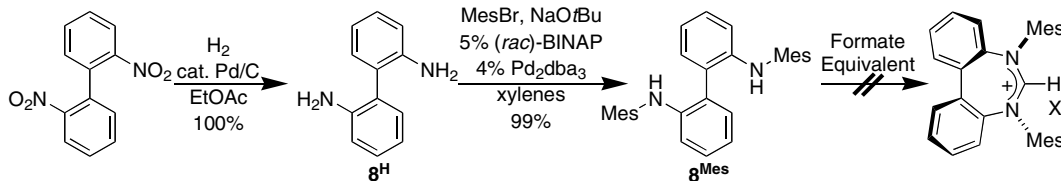


Fig. 2. Attempted synthesis of a 7-membered NHC-precursor amidinium salt bearing aryl nitrogen substituents.

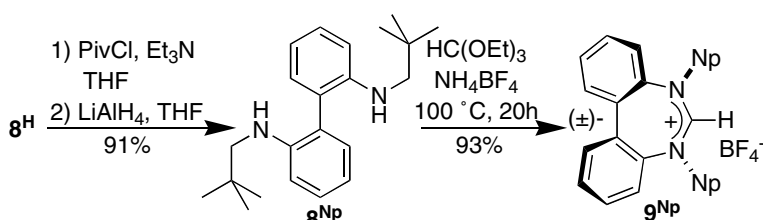


Fig. 3. Synthesis of a 7-membered NHC-precursor amidinium salt bearing alkyl nitrogen substituents.

salt, 9^{Np} , also proved to be an ineffective precursor for in situ preparation of an NHC–metal complex by deprotonation in the presence of a transition metal (vide infra).

The variant of 9^{Np} derived from enantiomerically resolved 2,2'-diamino-1,1'-binaphthyl was also prepared. The salt, 10^{Np} , was isolated in reasonable yield by using the same procedure as that used for 9^{Np} (Fig. 5) [15]. Unfortunately, attempts to obtain the free carbene derived from 10^{Np} were similarly unsuccessful.

Reasoning that increased steric bulk of the *N*-alkyl group could enhance the stability of the free carbene, we targeted more-sterically encumbered derivatives of 9^{H} (Fig. 6). Access to diamine 8^{H} was achieved in quantitative yield by condensation of 8^{H} with 2-adamantanone followed by reduction with LAH. The reaction of $8^{2\text{-Ad}}$ with triethylorthoformate produced $9^{2\text{-Ad}}$ [16], albeit in diminished yield compared to 9^{Np} . The somewhat lower yield in this reaction may reflect the increase in steric bulk of the 2-adamantyl groups. To date, we have been unable to prepare the enantiomerically resolved binaphthyl derivative of $9^{2\text{-Ad}}$ starting from 2,2'-diamino-1,1'-binaphthyl. The difficulty in preparing this derivative may arise from the fact that contraction of the biaryl torsional angle, which is necessary to achieve condensation with the formate reagent, is more restricted for binaphthyl than biphenyl.

2.3. Preparation of metal complexes possessing seven-membered NHC ligands

Our interest in palladium-catalyzed reactions prompted us to target the synthesis of NHC–Pd complexes derived from 9^{Np} . Unfortunately, standard procedures for the preparation of NHC-coordinated palladium complexes [1a,1b] were unsuccessful when $[\text{Pd}(\text{allyl})\text{Cl}]_2$, $\text{Pd}(\text{OAc})_2$, and PdCl_2 were used as the palladium reagent. A procedure outlined by Herrmann et al. [17] for the synthesis of an

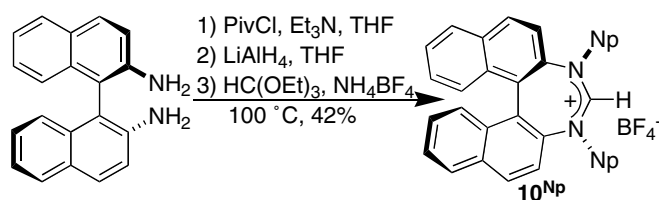


Fig. 5. Synthesis of an enantiomerically resolved amidinium salt.

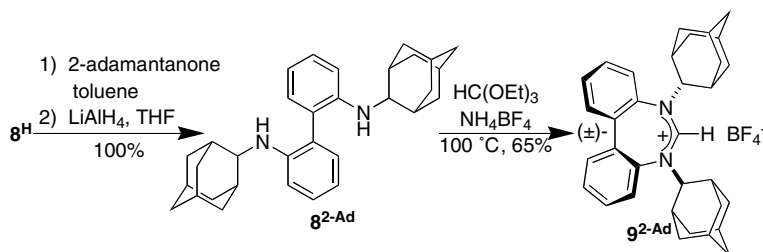


Fig. 6. Synthesis of a sterically encumbered 7-membered NHC-precursor amidinium salt bearing 2-adamantyl substituents attached to nitrogen.

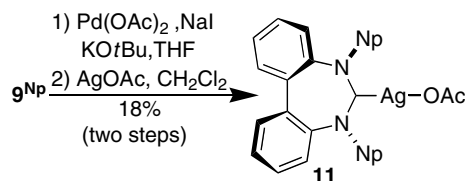


Fig. 7. Synthesis of NHC–Ag(I) complex **11**.

$[(\text{NHC})\text{Pd}(\text{I})_2]_2$ complex, however, yielded a semi-solid product, and crude ^1H NMR spectroscopic data revealed the disappearance of the amidinium proton resonance and was consistent with the presence of a carbene-containing product. After several unsuccessful attempts to isolate the adduct, we added AgOAc to a solution of the crude product with the hope of preparing an $(\text{NHC})\text{Pd}(\text{OAc})_2$ complex. Instead, we obtained the $(\text{NHC})\text{AgOAc}$ complex, **11**, from this reaction (Fig. 7). MALDI-TOF mass spectrometry revealed the presence of an $[\text{Ag}^{\text{I}}(\text{NHC})_2]^+$ cation, whereas X-ray analysis [16] (Fig. 8) revealed the linear $(\text{NHC})\text{Ag}^{\text{I}}(\kappa^1\text{-OAc})$ complex. These and previously reported results [18] supports the presence of an equilibrium in solution between the disproportionation salt, $[(\text{NHC})_2\text{-Ag}^{\text{I}}]$ $[\text{Ag}^{\text{I}}(\text{OAc})_2]$, and the $(\text{NHC})\text{Ag}^{\text{I}}(\text{OAc})$ complex (Fig. 9), where $(\text{NHC})\text{Ag}^{\text{I}}(\text{OAc})$ is the least soluble of the two species in hydrocarbon solvents. As further evidence of this equilibrium in solution, the carbene carbon resonance does not show coupling to the silver(I) nucleus [18].

Silver(I)–NHC complexes have been shown to act as carbene transfer agents to other transition metals, including Pd^{II} salts [19]. Interestingly, these data suggest the putative $[(\text{NHC})\text{Pd}(\text{I})_2]_2$ complex effects carbene transfer to Ag^{I} . Nonetheless, because Ag^{I} complexes of NHCs have been shown to act as carbene transfer agents to other transition metals, we attempted numerous alternative rational syntheses of **11**. Unfortunately, all such attempts failed. In addition, the preparation of metal complexes from the binaphthyl analog, 10^{Np} , have been similarly unsuccessful. Based on these observations, we conjecture that the steric protection imparted by the relatively small neopentyl substituents may be insufficient to stabilize a free carbene and to prepare stable NHC–metal complexes from these amidinium precursors.

In contrast to the difficulties we encountered in synthesizing metal complexes from 9^{Np} and 10^{Np} , $9^{2\text{-Ad}}$ afforded ready access to palladium(II) complexes. Synthesis of $(\text{NHC})\text{Pd}(\text{allyl})\text{Cl}$ (**12**) [16] by in situ deprotonation of

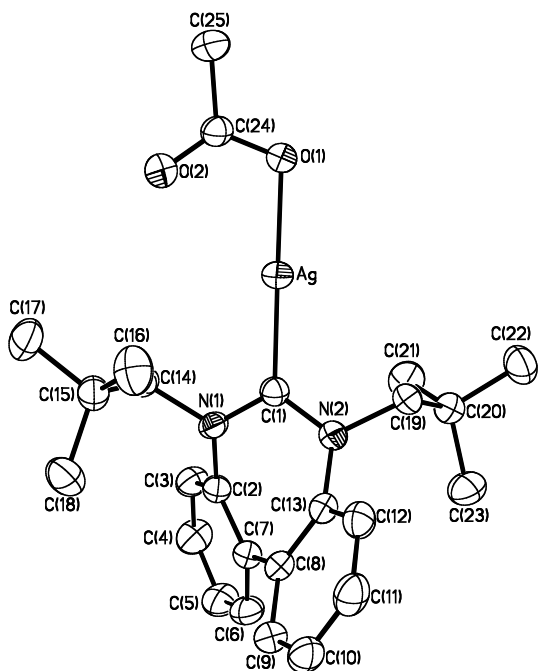


Fig. 8. Solid-state molecular structure of **11**. Hydrogen atoms and solvent are omitted for clarity. Thermal ellipsoids are shown at 50% probability. Selected bond lengths (Å) and angles (°): C1–Ag 2.0904(18), O1–Ag 2.1017(13), C1–N1 1.346(2), C1–N2 1.354(2), N1–C2 1.450(2), N2–C13 1.456(2), C2–C7 1.391(3), C13–C8 1.397(3), C7–C8 1.473(3); N1–C1–N2 117.74(16), C1–Ag–O1 179.35(6), C2–C7–C8–C13 41.1(3).

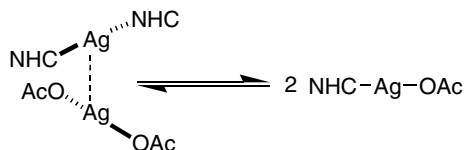


Fig. 9. Proposed equilibrium mixture of $[(\text{NHC})_2\text{Ag}^+][\text{Ag}^+(\text{OAc})_2^-]$ and $(\text{NHC})\text{Ag}^+(\text{OAc})$ (**11**) in solution.

9^{2-Ad} in the presence of $[\text{Pd}(\text{allyl})\text{Cl}]_2$ [20] proceeded in high yield (Fig. 10). The stability of this complex is demonstrated by its purification via silica gel chromatography under ambient conditions. $[(\text{NHC})\text{Pd}(\text{Cl})_2]_2$ (**13**) [16] was prepared in quantitative yield by protonolysis of the allyl ligand from $(\text{NHC})\text{Pd}(\text{allyl})\text{Cl}$ complex **12** [20]. Subjection of **13** to AgOAc or AgOCCF_3 in wet dichloromethane resulted in formation of the $(\text{NHC})\text{Pd}(\text{carboxylate})_2$ compounds, **14** and **15**, respectively (Fig. 10) [10a], each of which was characterized by single-crystal X-ray crystallography [16,21] (Figs. 11 and 12). Such species are attractive because $(\text{NHC})\text{Pd}(\text{O}_2\text{CR})_2(\text{OH}_2)$ complexes have found utility as catalysts both for alcohol oxidation [10] and Wacker-type oxidative cyclization [22]. Interestingly, both **14** and **15** exhibit intermolecular hydrogen bonding between the protons on the aqua ligand and the carbonyl oxygens of the carboxylate ligands in the solid state (Fig. 13). This solid-state structure contrasts the previously reported $(\text{NHC})\text{Pd}(\text{carboxylate})_2(\text{OH}_2)$ complexes, which exhibit *intramolecular* hydrogen bonding between the protons on the water ligand the carboxylate carbonyl oxygen atoms [10,23].

2.4. Identification and reactivity studies of NHC–alcohol adducts

Attempts to isolate the free carbene **16^{2-Ad}** by deprotonation of rigorously dried **9^{2-Ad}** with carbonate, hydride (with and without catalytic alkoxide), carbanion, or amide bases were again unsuccessful, producing only decomposition products. When alkoxide bases were employed, alcohol adducts of the free carbene were observed by ¹H NMR spectroscopy [24]. Stirring of the tertiary butanol adduct of **16^{2-Ad}** in THF in the presence of $[\text{Pd}(\text{allyl})\text{Cl}]_2$ did not result in formation of **12**. Similarly, the methanol

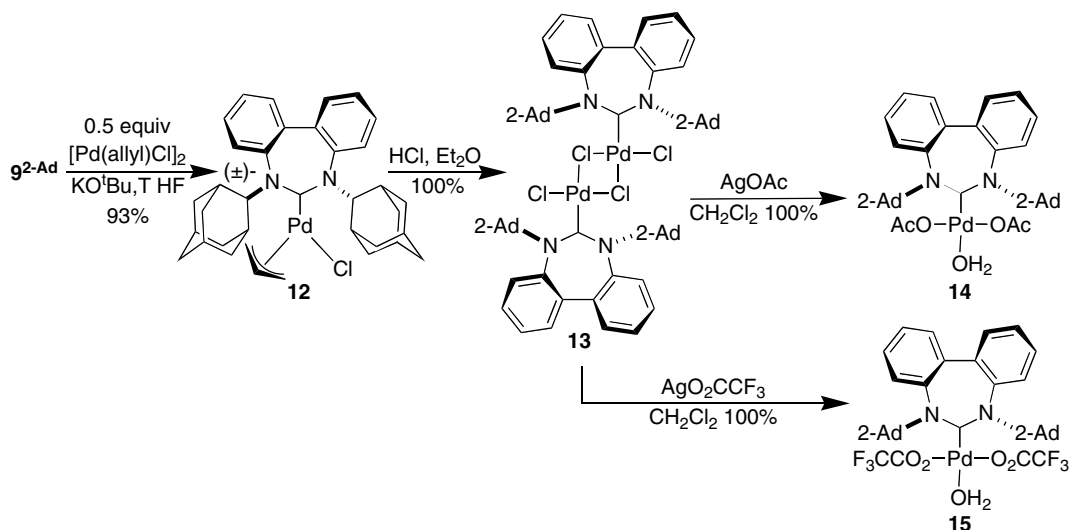


Fig. 10. Synthesis of four Pd(II) complexes bearing sterically hindered 7-membered NHC ligands.

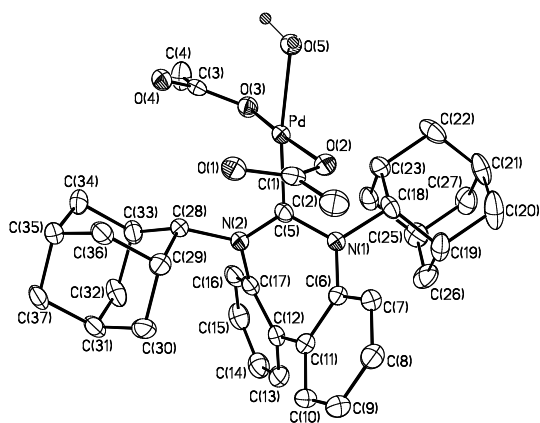


Fig. 11. Solid-state molecular structure of **14**. All H atoms except those on the water ligand have been omitted for clarity. Thermal ellipsoids are shown at 50% probability. Selected bond lengths (Å) and angles (°): Pd–C5 1.932(2), Pd–O2 2.0189(17), Pd–O3 2.0215(17), Pd–O5 2.1207(16); C5–Pd–O2 89.73(8), C5–Pd–O3 89.31(8), C5–Pd–O5 172.09(8), O2–Pd–O3 175.08(7).

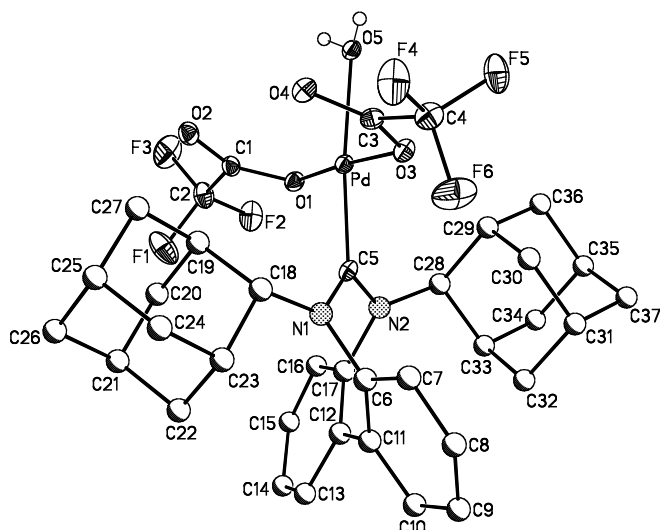


Fig. 12. Solid-state molecular structure of **15**. 50% probability ellipsoids are shown for atoms refined anisotropically (see Section 4, [21]). All H atoms except those on the water ligand are omitted for clarity. Only the preferred orientation of the carbene ligand is shown. Selected bond lengths (Å) and angles (°): Pd–C5 1.955(7), Pd–O1 2.037(5), Pd–O3 2.024(5), Pd–O5 2.141(5); C5–Pd–O1 87.4(2), C5–Pd–O3 89.9(2), C5–Pd–O5 173.1(2), O1–Pd–O3 176.1(2).

adduct of **16**^{2-Ad} does not react with [Pd(allyl)Cl]₂ to form **12** (Fig. 14). These observations suggest that in the synthesis of the NHC–palladium adduct, **12**, in situ deprotonation of **9**^{2-Ad} forms the free carbene **16**^{2-Ad}, which reacts with [Pd(allyl)Cl]₂.

2.5. Torsional distortion of the seven-membered heterocyclic framework

A unique aspect of this NHC framework is the presence of a torsionally twisted structure. This twist alleviates ring

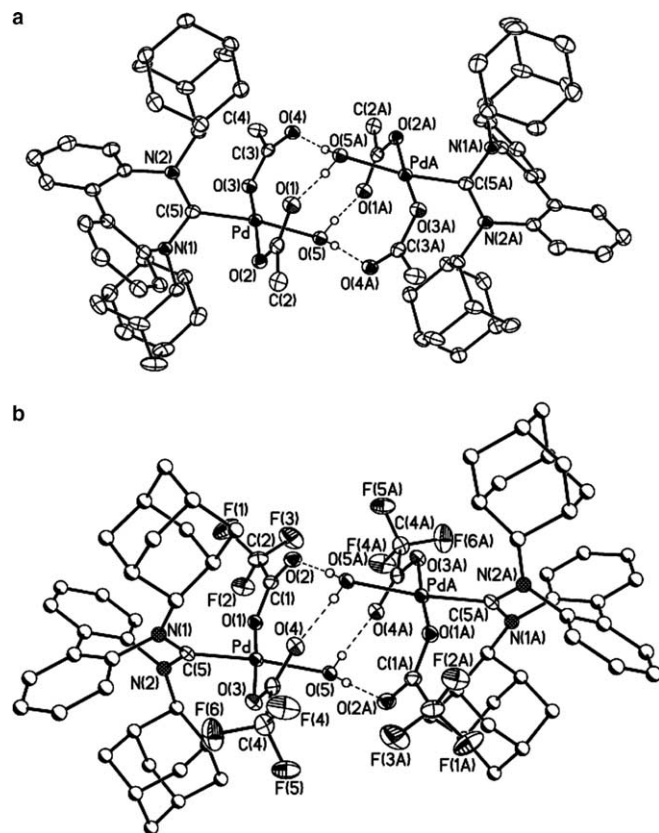


Fig. 13. Intermolecular hydrogen bonding in the solid state for **14** (a) and **15** (b).

strain associated with the seven-membered ring framework and provides Möbius stabilization of the formally antiaromatic 8 π -electron system (vide infra). We have evaluated metrics derived from crystal structures to assess the degree of this torsional twist, and we have defined two parameters, α and β . The former corresponds to the dihedral angle (α) between the two aryl rings of the biphenyl backbone. The latter describes the torsional angle (β) between the two N–C^R bonds (i.e., C–N \cdots N–C) [12] (Table 1); this parameter reflects the spatial disposition of the nitrogen substituents directed into the metal coordination sphere. Amidinium salt **9**^{2-Ad} exhibits an angle α greater than that of **9**^{Np} by 5.5°, possibly as a result of the larger steric bulk of 2-adamantyl groups over neopentyl groups. The larger β angle in **9**^{2-Ad} compared to **9**^{Np} is likely also a result of the larger steric bulk of 2-adamantyl compared to neopentyl. Interestingly, the amidinium salt, **9**^{Np}, and the linear (NHC)AgOAc complex, **11**, exhibit very similar torsional parameters. In contrast, significant differences in the β parameter are observed for the amidinium salt and palladium complexes that possess 2-adamantyl substituents. The magnitude of β seems to increase with increasing size and/or number of ligands in the coordination sphere. These observations suggest that the *cis* substituents in the palladium complexes exert significant influence on the distortion of the carbene ligand.

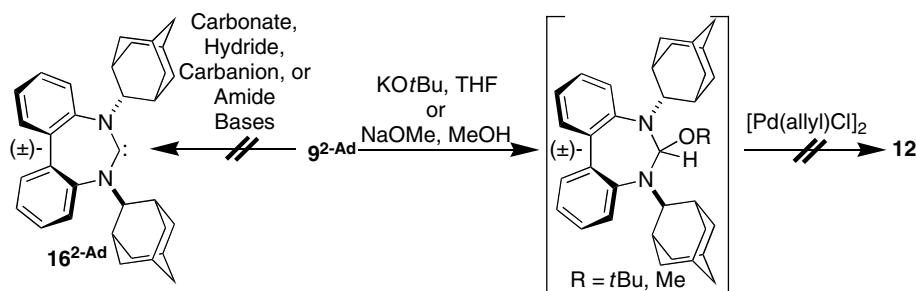


Fig. 14. Reactivity of amidinium salts with various bases.

Table 1

Comparison of the torsional angles, α and β (defined in text), for amidinium salts and metal complexes of the 7-membered NHC

Structure	α	β
Amidinium salt, 9^{Np}	40.6(2)°	62.3(2)°
Amidinium salt, 9^{2-Ad}	46.1(4)°	56.2(5)°
NHC–Ag–OAc, 11	41.1(3)°	61.9(3)°
NHC–Pd(allyl)Cl, 12	41.9(5)°	72.3(8)°
[NHC–Pd(Cl) ₂] ₂ , 13	46.4(8)°	79.7(13)°
NHC–Pd(OAc) ₂ (OH) ₂ , 14	39.3(3)°	91.9(4)°

2.6. Electronic structure analysis of seven-membered N-heterocyclic carbenes

Seven-membered N-heterocyclic carbenes were unprecedented prior to our initial report [12]; however, Rzepa and co-workers [25] had published an earlier computational analysis of related structures, including 7^{CH_3} . Their study probed the contribution of Möbius aromaticity [26] to stabilization of the 8π -electron seven-membered ring. Our own DFT calculations of 7^{CH_3} reproduces the twisted conformation of the carbene (Fig. 15) and reveals a biphenyl dihedral angle (α) of 44.7° that agrees well with our experimentally determined geometries (**11**, Fig. 8). The β value, however, is only 23.6°, possibly reflecting the small size of the methyl groups.

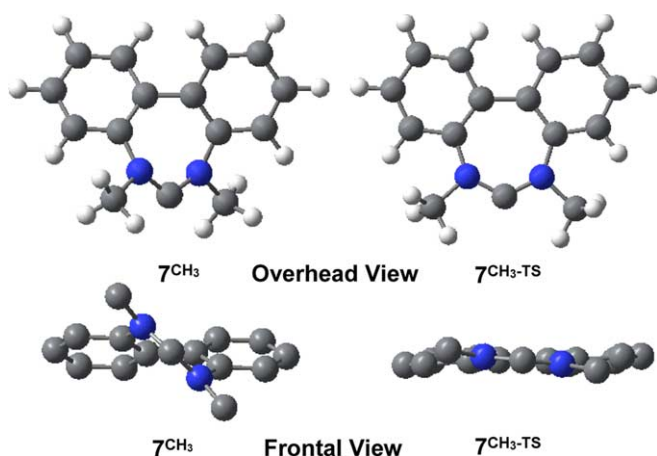


Fig. 15. Computationally-derived ground- and transition-state structures of a 7-membered NHC.

In order to probe the aromaticity of the 7-membered ring, we used the method of “nucleus independent chemical shifts” (NICSs) developed by Schleyer et al. [27]. Initial calculation of the NICS value at the 7-membered ring center-of-mass (COM) of 7^{CH_3} led to a value of 6.7 ppm that agrees well with the previously computed NICS value reported for 7^{CH_3} by Rzepa and co-workers [25] of 6.9 ppm. The positive magnitude of the COM NICS value suggests that the free carbene possesses a formal antiaromatic electronic configuration.

Rzepa and co-workers [25] examined the effects of complexing 7^{CH_3} to a palladium center and their calculations suggest that the barrier to thermal racemization of bound 7^{CH_3} is greater than 20 kcal/mol. We wanted to evaluate this barrier in the free carbene with the aim to assess the extent to which the Möbius ring twist contributes to an overall decrease in antiaromaticity in the free carbene. The geometry of a flat 7-membered ring corresponding to 7^{CH_3} was optimized to a transition state structure (7^{CH_3-TS}) with exactly one negative vibrational mode (Fig. 15). 7^{CH_3-TS} lies 12.7 kcal/mol higher in energy and if this value models the atropisomeric inversion barrier, it suggests that thermal racemization of the free carbene will be facile at room temperature. The NICS value computed at the COM for 7^{CH_3-TS} , 11.7 ppm, is significantly higher than that of the twisted structure and highlights the stabilization associated with a Möbius ring twist in 7^{CH_3} .

The use of NICS values to measure the diatropic (aromatic) versus paratropic (antiaromatic) induced ring currents at the ring COM has become a well-established computational technique. Shortly after reporting the COM NICS technique, Schleyer analyzed the total NICS value based on the contributions from the diatropic and paratropic components and suggested that the NICS value be calculated at 1 Å above the ring COM in order to minimize local electronic effects [28]. This suggestion prompted us to reevaluate the NICS value as a function of distance

Table 2
NICS value (ppm) as a function of distance above the ring center

	0 Å (COM)	0.5 Å	1 Å	2 Å	3 Å
7^{CH_3}	6.7	4.2	1.2	0.3	0
7^{CH_3-TS}	11.7	10.1	7.1	2.3	0.6

above the 7-membered ring center of 7^{CH_3} and $7^{\text{CH}_3\text{-TS}}$ (Table 2). The resulting NICS value of 1.2 ppm (essentially non-aromatic) for 7^{CH_3} at 1 Å above the ring center suggests that the torsional twist effectively cancels the antiaromatic contribution to the overall electronic structure. A decrease in the magnitude of the NICS value is also observed for $7^{\text{CH}_3\text{-TS}}$ at 1 Å relative to the COM calculation (Table 2); however, the positive value of 7.1 ppm reveals that significant antiaromatic character remains.

This computational analysis indicates that evaluating the true magnitude of the antiaromatic character of 7^{CH_3} and $7^{\text{CH}_3\text{-TS}}$ is non-trivial; however, it is clear that Möbius aromatic stabilization occurs in structures with the framework of **7**. Further analysis of the individual NICS components will be necessary in order to define the total NICS value and consequently the antiaromaticity of the ring systems.

3. Conclusions

The studies outlined above demonstrate that expansion of the heterocyclic core of an NHC ligand to encompass a seven-membered ring causes the structure to deviate significantly from a planar geometry. The torsional twist in the seven-membered amidinium salts and corresponding metal-coordinated carbenes results in axially chiral, C_2 -symmetric structures that point toward their utility in asymmetric catalysis. Toward this end, our current studies are focusing on the preparation of enantiomerically resolved analogs of these compounds. Another important focus of our ongoing studies is the preparation of more stable derivatives that will enable the isolation of stable carbenes, a goal that has, thus far, been elusive.

4. Experimental

4.1. General

All manipulations were performed under an inert nitrogen atmosphere unless otherwise specified. Dry, oxygen-free solvents were employed. ^1H and ^{13}C NMR spectra were recorded on a Bruker Phoenix-250, Bruker Homer-300, Varian Mercury-300, Varian Unity-500, or a Varian Inova-500 NMR spectrometer. ^1H chemical shifts are reported in ppm relative to Me_4Si as an external standard, while ^{13}C chemical shifts are reported in ppm relative to solvent.

4.2. Structural determination of 9^{Np} , **11**, **14**, and **15**

Crystals suitable for X-ray diffraction were obtained as follows: 9^{Np} : 9^{Np} (ca. 10 mg) was dissolved in minimal chloroform. Vapor diffusion of *n*-pentane onto the chloroform solution afforded crystals after 1 day. **11**:**11** (ca. 10 mg) was taken up in minimal toluene. The volume of toluene was then doubled. Vapor diffusion of *n*-pentane onto the toluene solution afforded crystals after 1–2 days. **14** and **15**:

ca. 10 mg was dissolved in minimal diethyl ether, the volume of ether was doubled, and the solution was cooled to -20°C . Warm *n*-heptane was layered onto the -20°C ethereal solution. Overnight diffusion of the liquids at -20°C afforded small yellow crystals.

See Table 3. A colorless (9^{Np} and **11**) or yellow (**14** and **15**) crystal was selected under oil under ambient conditions and attached to the tip of a nylon loop. The crystal was mounted in a stream of cold nitrogen at 100(2) K (9^{Np} , **14**, and **15**) or 200(2) K (**11**) and centered in the X-ray beam by using a video camera.

The crystal evaluation and data collection were performed on a Bruker CCD-1000 diffractometer with $\text{Mo K}\alpha$ ($\lambda = 0.71073 \text{ \AA}$) radiation and the diffractometer to crystal distance of 4.9 cm.

The initial cell constants were obtained from three series of ω scans at different starting angles. Each series consisted of 20 frames collected at intervals of 0.3° in a 6° range about ω with the exposure time of 10 (9^{Np} , **14**, and **15**) or 15 (**11**) seconds per frame. A total of 121 (9^{Np} and **15**), 206 (**11**), or 76 (**14**) reflections were obtained. The reflections were successfully indexed by an automated indexing routine built in the SMART program. The final cell constants were calculated from a set of 8632 (9^{Np}), 10,935 (**11**), 11,009 (**14**), or 9536 (**15**) strong reflections from the actual data collection.

The data were collected by using the hemisphere (9^{Np} and **11**) data collection routine or the full sphere (**14** and **15**) data collection routine to survey the reciprocal space to the extent of a full sphere to a resolution of 0.80 Å. A total of 11,013 (9^{Np}), 24,283 (**11**), 30,455 (**14**), or 27,822 (**15**) data were harvested by collecting three sets of frames with 0.3° (9^{Np} , **14**, and **15**) or 0.25° (**11**) scans in ω with an exposure time 24 s (9^{Np}), 25 s (**11**), or 36 s (**14** and **15**) per frame. These highly redundant datasets were corrected for Lorentz and polarization effects. The absorption correction was based on fitting a function to the empirical transmission surface as sampled by multiple equivalent measurements [29].

A successful solution by the direct methods provided most non-hydrogen atoms from the *E*-map. The remaining non-hydrogen atoms were located in an alternating series of least-squares cycles and difference Fourier maps. All non-hydrogen atoms were refined with anisotropic displacement coefficients unless specified otherwise. All hydrogen atoms were included in the structure factor calculation at idealized positions and were allowed to ride on the neighboring atoms with relative isotropic displacement coefficients.

In the case of 9^{Np} , there is also a solvent molecule of chloroform in the asymmetric unit.

In the case of **11**, there is a toluene solvent molecule which is equally disordered over two positions and was refined with soft restraints and constraints.

In the case of **14**, there were two solvent molecules of dichloromethane and/or ether present in the asymmetric unit. A significant amount of time was invested in identifying

Table 3
Crystallographic data for reported complexes

Complex	9 ^{Np}	11	14	15
Empirical formula	[C ₂₃ H ₃₁ N ₂][BF ₄] · CHCl ₃	AgC ₂₅ H ₃₄ N ₂ O ₂ · C ₇ H ₈	C ₃₇ H ₄₆ N ₂ O ₅ Pd · 2CH ₂ Cl ₂	C ₃₇ H ₄₀ F ₆ N ₂ O ₅ Pd
Formula weight	541.68	593.54	875.01	813.11
Temperature (K)	273(2)	200(2)	100(2)	100(2)
Wavelength (Å)	0.71073	0.71073	0.71073	0.71073
Crystal system	Monoclinic	Monoclinic	Monoclinic	Monoclinic
Space group	<i>P</i> 2 ₁	<i>P</i> 2 ₁ / <i>n</i>	<i>C</i> 2/ <i>c</i>	<i>P</i> 2 ₁ / <i>n</i>
Unit cell dimensions				
<i>a</i> (Å)	8.9030(4)	12.2161(18)	28.5870(15)	10.6966(7)
<i>b</i> (Å)	14.4914(7)	13.603(2)	14.6415(8)	18.7371(12)
<i>c</i> (Å)	10.6132(5)	18.526(3)	19.8079(11)	17.0145(11)
α(°)	90	90	90	90
β(°)	106.0570(10)	102.401(2)	115.736(1)	95.650(1)
γ(°)	90	90	90	90
Volume (Å ³)	1315.86(11)	3006.7(8)	7468.3(7)	3393.5(4)
<i>Z</i>	2	4	8	4
Density (calculated) (Mg/m ³)	1.367	1.311	1.556	1.591
Absorption coefficient (mm ⁻¹)	0.392	0.699	0.831	0.627
<i>F</i> (000)	564	1240	3616	1664
Crystal size (mm ³)	0.37 × 0.36 × 0.33	0.29 × 0.23 × 0.19	0.36 × 0.25 × 0.18	0.47 × 0.26 × 0.23
θ Range for data collection (°)	2.38–26.40	2.24–26.44	1.60–26.40	2.16–26.39
Index ranges	–11 ≤ <i>h</i> ≤ 11; –18 ≤ <i>k</i> ≤ 18; –13 ≤ <i>l</i> ≤ 13	–15 ≤ <i>h</i> ≤ 15; –16 ≤ <i>k</i> ≤ 17; –23 ≤ <i>l</i> ≤ 23	–35 ≤ <i>h</i> ≤ 35; –18 ≤ <i>k</i> ≤ 17; –24 ≤ <i>l</i> ≤ 24	–13 ≤ <i>h</i> ≤ 13; –23 ≤ <i>k</i> ≤ 23; –21 ≤ <i>l</i> ≤ 21
Reflections collected	11,013	24,283	30,455	27,822
Independent reflections (<i>R</i> _{int})	5288 (0.0186)	6155 (0.0296)	7613 (0.0365)	6950 (0.0246)
Completeness to theta, % (°)	99.8 (26.40)	99.5 (26.44)	99.2 (26.40)	99.8 (26.39)
Maximum and minimum transmission	0.8814 and 0.8684	0.8786 and 0.8229	0.8649 and 0.7542	0.8692 and 0.7570
Refinement method	Full-matrix least-squares on <i>F</i> ²	Full-matrix least-squares on <i>F</i> ²	Full-matrix least-squares on <i>F</i> ²	Full-matrix least-squares on <i>F</i> ²
Data/restraints/parameters	5288/1/313	6155/12/383	7613/3/414	6950/135/320
Goodness-of-fit on <i>F</i> ²	1.041	1.042	1.048	1.042
Final <i>R</i> indices [<i>I</i> > 2σ(<i>I</i>)]	<i>R</i> ₁ = 0.0250; <i>wR</i> ₂ = 0.0630	<i>R</i> ₁ = 0.0273; <i>wR</i> ₂ = 0.0684	<i>R</i> ₁ = 0.0346; <i>wR</i> ₂ = 0.0916	<i>R</i> ₁ = 0.1036; <i>wR</i> ₂ = 0.2624
<i>R</i> indices (all data)	<i>R</i> ₁ = 0.0258; <i>wR</i> ₂ = 0.0638	<i>R</i> ₁ = 0.0335; <i>wR</i> ₂ = 0.0719	<i>R</i> ₁ = 0.0436; <i>wR</i> ₂ = 0.0960	<i>R</i> ₁ = 0.1078; <i>wR</i> ₂ = 0.2659
Largest difference in peak and hole (e Å ⁻³)	0.478 and –0.335	0.449 and –0.182	0.888 and –0.287	3.179 and –2.338

and refining the disordered molecules. Bond length restraints were applied to model the molecules but the resulting isotropic displacement coefficients suggested the molecules were mobile. In addition, the refinement was computationally unstable. Option SQUEEZE of program PLATON [30] was used to correct the diffraction data for diffuse scattering effects and to identify the solvate molecule. PLATON calculated the upper limit of volume that can be occupied by the solvent to be 1558 Å³, or 21% of the unit cell volume. The program calculated 689 electrons in the unit cell for the diffuse species. This approximately corresponds to two molecules of dichloromethane per Pd complex in the asymmetric unit (672 electrons). It is very likely that these solvate molecules are disordered over several positions. Note that all derived results in the following table are based on the known contents. No data are given for the diffusely scattering species.

In the case of **15**, the carbene ligand is disordered over two positions in a 63:37 ratio and was refined with an idealized geometry. All atoms of the carbene ligand were refined isotropically. The ligand disorder resulted in multiple positions of the adamantyl groups. Two positions for each group were identified and refined. The residual peaks of electron density suggested that a third orientation for each adamantyl group could be present. After considerable effort was spent on identifying and refining the third locations it was decided that these orientations of the adamantyl group did not clearly correspond to chemically reasonable positions and their incorporation into the model resulted in only slight overall improvement of the structural refinement. Thus, the possible third positions were ignored and only two positions for each adamantyl substituent are presented.

4.3. 2,2'-Diaminobiphenyl **8^H**

2,2'-Dinitrobiphenyl **1** (102.0 g, 417.5 mmol) and 10% Pd/C (16.4 g) were combined with 300 mL EtOAc in a hydrogenation vessel. The vessel was pressurized to 40 psi H₂ for 3.5 h (when H₂ was no longer being consumed). The slurry was filtered through a plug of celite. Rotary evaporation followed by drying on a vacuum line gave pure product as a light yellow/orange powder in 100% yield. ¹H NMR (CDCl₃, 297 K, 300 MHz): δ 3.71 (s, 4H), δ 6.79 (dd, 2H, *J* = 8.0, 1.2 Hz), δ 6.84 (td, 2H, *J* = 7.5, 1.2 Hz), δ 7.12 (dd, 2H, *J* = 8.1, 1.5 Hz), δ 7.19 (ddd, 2H, *J* = 7.2, 1.5, 0.6 Hz). ¹³C NMR (CDCl₃, 297 K, 300 MHz): δ 115.58, δ 118.71, δ 124.62, δ 128.81, δ 131.08, δ 144.22. HRMS (*m/z*): calculated 185.1078, measured 185.1073.

4.4. 2,2'-Bis(pivaloylamino)-1,1'-biphenyl **8^{Piv}**

Compound **8^{Piv}** was synthesized by an adaptation of a literature procedure [15]. **8^H** (6.50 g, 35.3 mmol) was weighed into an oven-dried 100 mL rbf equipped with a stir bar and a septum-capped condenser, followed by N₂ purging. The system was charged with 70 mL dry THF

and TEA (15.2 mL, 109 mmol). Pivaloyl chloride (11.3 mL, 91.7 mmol) was added dropwise via syringe to the above stirred solution, yielding a white precipitate. System was heated to reflux (ca. 80 °C) for 3 h under a N₂ atmosphere. The precipitate was filtered and washed with THF. Filtrate and washes were combined and liquids removed on a rotary evaporator giving pure **8^{Piv}** as a white powder in 100% yield. ¹H NMR (CDCl₃, 297 K, 300 MHz): δ 1.00 (s, 18H), δ 7.18 (s, 2H), δ 7.24 (m, 4H), δ 7.46 (m, 2H), δ 8.32 (d, 2H, *J* = 8.2 Hz). ¹³C NMR (CDCl₃, 297 K, 250 MHz): δ 27.33, δ 39.80, δ 122.15, δ 124.79, δ 128.36, δ 129.76, δ 129.94, δ 136.25, δ 176.90. HRMS (*m/z*): calculated 375.2048, measured 375.2060.

4.5. 2,2'-Bis(neopentylamino)-1,1'-biphenyl **8^{Np}**

Compound **8^{Np}** was synthesized by an adaptation of a literature procedure [15]. An oven-dried 500 mL rbf equipped with a stir bar was charged with LAH (8.03 g, 211 mmol) in a dry box. Reaction vessel was capped with a septum, and 300 mL dry THF was added via syringe (outside of dry box). In a 100 mL oven-dried rbf, **8^{Piv}** (12.44 g, 35.3 mmol) was dissolved in 200 mL dry THF under N₂, which was then slowly cannula transferred to the stirred LAH suspension. To the reaction vessel was attached an oven-dried septum-capped condenser with a N₂ inlet. The suspension was heated to reflux (ca. 80 °C) for 3.5 days, followed by careful quenching with H₂O until fizzing ceased to be visible. 2 M NaOH(aq) was added until a clear THF layer could be seen. The slurry was filtered and the solid washed with THF. The layers were separated and the aqueous layer was washed twice with 200 mL THF. Organic layers were combined, dried over MgSO₄, and solvent removed to yield a mixture primarily consisting of starting material and product. The product was isolated as a clear oil in 91% yield by column chromatography (SiO₂, 7.5% EtOAc in hexanes). ¹H NMR (CDCl₃, 297 K, 300 MHz): δ 0.82 (s, 18H), δ 2.84 (m, 4H), δ 3.68 (t, 2H, *J* = 5.1 Hz), δ 6.73 (m, 4H), δ 7.09 (m, 2H), δ 7.24 (m, 2H). ¹³C NMR (CDCl₃, 297 K, 250 MHz): δ 27.8, δ 32.1, δ 55.8, δ 110.2, δ 116.6, δ 123.7, δ 129.2, δ 130.8, δ 146.8. HRMS (*m/z*): calculated 325.2643, measured 345.2656.

4.6. Amidinium tetrafluoroborate salt **9^{Np}**

Compound **8^{Np}** (10.3 g, 32.0 mmol) and NH₄BF₄ (3.36 g, 32.1 mmol) were combined in a 500 mL rbf equipped with a stir bar and topped with a condenser. 20 mL of triethyl orthoformate was added and the system was heated to ca. 100 °C for 20 h. After cooling to room temperature, pentane was added (ca. 100 mL). The suspension was filtered, and the crystals washed with pentane to give **9^{Np}** as a white powdery solid in 93% yield. Crystals suitable for X-ray analysis were achieved by vapor diffusion of *n*-pentane onto a CHCl₃ solution of **9^{Np}**. ¹H NMR (CDCl₃, 297 K, 300 MHz): δ 0.77 (s, 18H), δ 4.00

(s, 4H), δ 7.38 (m, 2H), δ 7.51 (m, 6H), δ 8.83 (s, 1H). ^{13}C NMR (CDCl_3 , 297 K, 300 MHz): δ 27.1, δ 34.0, δ 66.4, δ 122.9, δ 130.0, δ 130.4, δ 130.6, δ 132.8, δ 146.3, δ 171.3. HRMS (m/z): calculated 335.2487, measured 335.2495.

4.7. (*R*)-2,2'-bis(pivaloylamino)-1,1'-binaphthyl

(*R*)-2,2'-bis(pivaloylamino)-1,1'-binaphthyl was synthesized according to a literature procedure [15]. An oven-dried 100 mL rbf fitted with a reflux condenser was charged with 500 mg (1.8 mmol) (*R*)-(+)-2,2'-diaminobinaphthyl and 760 μL (5.45 mmol) TEA. 10 mL of dry THF was cannula transferred into the reaction vessel, followed by syringe addition of 560 μL (4.6 mmol) pivaloyl chloride. The reaction mixture was refluxed 2 h, then filtered. The volatiles were removed leaving pure product in 100% yield as an off-white powder. ^1H NMR (CDCl_3 , 297 K, 300 MHz): δ 0.75 (s, 18H), δ 7.14 (br s, 2H), δ 7.18 (d, $J = 8.4$ Hz, 2H), δ 7.32 (ddd, $J = 8.4, 6.9, 1.2$ Hz, 2H), δ 7.46 (ddd, $J = 8.4, 6.9, 1.2$ Hz, 2H), δ 7.95 (d, $J = 8.4$ Hz, 2H), δ 8.05 (d, $J = 9.0$ Hz, 2H), δ 8.48 (d, $J = 9.0$ Hz, 2H).

4.8. (*R*)-2,2'-bis(neopentylamino)-1,1'-binaphthyl

(*R*)-2,2'-bis(neopentylamino)-1,1'-binaphthyl was synthesized according to a literature procedure [15]. 64% yield as an off-white powder. ^1H NMR (CDCl_3 , 297 K, 300 MHz): δ 0.67 (s, 18H), δ 2.94 (AMX pattern, 4H), δ 3.73 (t, $J = 6.0$ Hz, 2H), δ 7.00–7.03 (m, 2H), δ 7.11–7.17 (m, 4H), δ 7.25 (d, $J = 9.3$ Hz, 2H), δ 7.75 (m, 2H), δ 7.85 (d, $J = 9.0$ Hz).

4.9. Amidinium Salt 10^{Np}

See synthesis of 9^{Np} . Product did not crash out of reaction, but was purified by removing excess orthoester under vacuum, dissolving in minimal CH_2Cl_2 , and crashing out with pentane to give 10^{Np} in 65% yield as a light brown powder. ^1H NMR (CDCl_3 , 297 K, 300 MHz): δ 0.64 (s, 18H), δ 4.01 (d, $J = 13.8$ Hz, 2H), δ 4.20 (d, $J = 13.8$ Hz, 2H), δ 7.07 (d, $J = 8.4$ Hz, 2H), δ 7.34 (t, $J = 7.2$ Hz, 2H), δ 7.62 (m, 4H), δ 8.00 (d, $J = 8.1$ Hz, 2H), δ 8.12 (d, $J = 9.0$ Hz), δ 8.85 (s, 1H). ^{13}C NMR (CDCl_3 , 297 K, 300 MHz): δ 27.0, δ 33.9, δ 65.8, δ 120.2, δ 124.2, δ 126.4, δ 127.8, δ 128.1, δ 128.8, δ 131.5, δ 131.8, δ 132.9, δ 147.5, δ 173.1. HRMS (m/z): calculated 435.2800, measured 435.2794.

4.10. 2,2'-bis(2-adamantylamino)-1,1'-biphenyl $8^{2\text{-Ad}}$

614 mg (3.33 mmol) of 8^{H} and 1 g (6.65 mmol) 2-adamantanone were combined with 1% (per amine functionality) pTsOH in a Dean-Stark apparatus. The reagents were dissolved in ca. 200 mL toluene and refluxed for 72 h. The solvent was removed and 122 mg (3.22 mmol) LAH was added, followed by ca. 200 mL THF. The reaction flask was heated to 50 $^\circ\text{C}$ for 2 h then cooled on an ice

bath, followed by a careful quenching with ca. 100 mL water and 10 mL sat. NH_4BF_4 . The resulting slurry was filtered through a plug of celite, and the plug washed with CH_2Cl_2 . The aqueous layer was washed once with CH_2Cl_2 (ca. 100 mL). The organic layers were combined, dried over MgSO_4 , filtered, and the solvent was removed, yielding pure $8^{2\text{-Ad}}$ in 100% yield as an off-white powder. ^1H NMR (CDCl_3 , 297 K, 300 MHz): δ 1.38–1.97 (m, 28H), δ 3.54 (s, 2H), δ 4.05 (s, 2H), δ 6.71 (m, 4H), δ 7.11 (m, 2H), δ 7.22 (m, 2H). ^{13}C NMR (CDCl_3 , 297 K, 300 MHz): δ 27.4, δ 27.6, δ 31.3, δ 31.7, δ 31.8, δ 32.2, δ 37.4, δ 37.8, δ 37.9, δ 56.7, δ 111.1, δ 116.3, δ 124.0, δ 129.1, δ 130.9, δ 145.3. HRMS (m/z): calculated 453.3269, measured 453.3247.

4.11. Amidinium tetrafluoroborate salt $9^{2\text{-Ad}}$

5.76 g (12.7 mmol) $8^{2\text{-Ad}}$ and 1.3 g (12.7 mmol) NH_4BF_4 were combined under nitrogen in a 500 mL rbf, and ca. 200 mL triethyl orthoformate was added. The reaction was heated to 100 $^\circ\text{C}$ for 16 h, after which time the product had crashed out of solution as a white powder. The reaction cooled to room temperature, was filtered and the solid washed with diethyl ether followed by pentane to give the amidinium salt $9^{2\text{-Ad}}$ in 65% yield as a light fluffy white powder without further purification. ^1H NMR (CDCl_3 , 297 K, 300 MHz): δ 0.97 (d, 2H, $J = 13.0$ Hz), δ 1.14 (d, 2H, $J = 13.0$ Hz), δ 1.47–2.09 (m, 22H), δ 2.66 (s, 2H), δ 4.77 (s, 2H), δ 7.43 (m, 2H), δ 7.51 (m, 6H), δ 8.84 (s, 1H). ^{13}C NMR (CDCl_3 , 297 K, 300 MHz): δ 26.39, δ 26.74, δ 30.00, δ 30.11, δ 30.36, δ 31.71, δ 36.28, δ 36.38, δ 37.01, δ 65.55, δ 124.29, δ 129.48, δ 129.51, δ 129.56, δ 134.09, δ 143.97, δ 175.42. HRMS (m/z): calculated 463.3113, measured 463.3099.

4.12. NHC–Ag–OAc (**11**)

Compound 9^{Np} (524 mg, 1.24 mmol), NaI (778 mg, 5.19 mmol), KO^tBu (186 mg, 1.66 mmol), and $\text{Pd}(\text{OAc})_2$ (278 mg, 1.24 mmol) were combined in a schlenk flask under a nitrogen atmosphere. After cooling to -78 $^\circ\text{C}$, 15 mL dry THF was added, and the solution was stirred overnight as the temperature slowly warmed to room temperature. Solvent was removed in a dry box, and the residue was taken up in CH_2Cl_2 . Filtration through a plug of celite, followed by washing the plug with a small amount of CH_2Cl_2 gave a yellow/brown solution. Addition of AgOAc and stirring for 24 h gave a brown suspension with white ppt present. Filtration through celite, removal of solvent in vacuo, taking up in minimal CH_2Cl_2 and addition of excess hexanes gave a semi-cloudy light brown solution. Removal of small amount of solvent in vacuo promoted precipitation of an off-white solid, which was collected by filtration as pure **6** by NMR as a light tan powder in 18% yield. Crystals suitable for X-ray analysis were achieved by vapor diffusion of *n*-pentane onto a toluene solution of **11**. ^1H NMR (CDCl_3 , 297 K, 300 MHz): δ 0.58 (s, 18H),

δ 2.03 (s, 3H), δ 3.90 (d, 2H, $J = 13.4$ Hz), δ 4.20 (d, 2H, $J = 13.4$ Hz), δ 7.13 (m, 2H), δ 7.30 (m, 6H). ^{13}C NMR (CDCl_3 , 297 K, 500 MHz): δ 27.8, δ 33.9, δ 71.9, δ 123.3, δ 127.8, δ 128.8, δ 129.0, δ 135.4, δ 149.5, δ 179.3 (s, carbene). MALDI-TOF (m/z): 335.3 ($(\text{NHC-H})^+$), 441.0 ((NHC-Ag^+)), 774.9 ($(\text{NHC})_2\text{Ag}^+$).

4.13. *NHC-Pd(allyl)Cl* (**12**)

200 mg (0.363 mmol) of aminidinium salt **9**^{2-Ad} and 78 mg (0.213 mmol) $[\text{Pd}(\text{allyl})\text{Cl}]_2$ was combined with 1.2 eq of KO^tBu under nitrogen. The reaction was stirred in THF for 12 h, filtered through celite, and purified on a column under ambient conditions (SiO_2 , 1:1 Ether:Hexanes) to give the *NHC-Pd(Allyl)Cl* complex **11** in 93% yield as a light yellow-tan solid. Crystals suitable for X-ray analysis were achieved by layering *n*-pentane onto a -20°C toluene solution of **12**. ^1H NMR (CDCl_3 , 297 K, 500 MHz): δ 0.79–2.11 (m, 67.2H), δ 2.66 (s, 1.4H), δ 2.76 (d, 1.4H, $J = 11.0$ Hz), δ 3.16–3.31 (m, 4.8H), δ 3.52 (s, 1H), δ 3.76 (d, 1H, $J = 6.0$ Hz, 1H), δ 3.99–4.21 (m, 3.8H), δ 5.16 (m, 2.8H), δ 5.45 (m, 2H), δ 6.95 (m, 2.4H), δ 7.28–7.56 (m, 16.8H). ^{13}C NMR (CDCl_3 , 297 K, 500 MHz): δ 26.5, δ 26.6, δ 26.7, δ 26.8, δ 26.9, δ 29.9, δ 30.0, δ 30.09, δ 30.11, δ 30.2, δ 30.4, δ 30.5, δ 31.1, δ 31.2, δ 36.1, δ 36.8, δ 37.0, δ 37.1, δ 37.2, δ 37.4, δ 37.5, δ 43.3, δ 46.1, δ 66.5, δ 66.6, δ 66.7, δ 66.9, δ 71.2, δ 73.1, δ 115.2, δ 124.7, δ 125.0, δ 126.7, δ 126.8, δ 126.9, δ 127.0, δ 127.1, δ 127.2, δ 127.6, δ 136.3, δ 136.4, δ 137.1, δ 146.2, δ 146.4, δ 146.6, δ 147.1 (carbene carbons not detected). ESI-MS (m/z) (highest intensity peaks listed): 609.1 ($(\text{NHC-Pd}(\text{allyl})^+)$), 650.2 ($(\text{NHC-Pd}(\text{allyl})\text{Cl-Li}^+)$), 667.2 ($(\text{NHC-Pd}(\text{allyl})\text{Cl-Na}^+)$), 1255.3 ($([\text{NHC-Pd}(\text{allyl})_2\text{Cl}]^+)$).

4.14. $[\text{NHC-Pd}(\text{Cl})_2]$ (**13**)

A 50 mL rbf was charged with 100 mg (0.16 mmol) **12** and 2.0 mL 2.0 M ethereal HCl. The color instantly changed to bright yellow-orange. 8.0 mL ether was added and the resultant suspension stirred 1 h. Volatiles were removed in vacuo leaving pure **13** as a bright yellow-orange powder in quantitative yield. **13** could be recrystallized by taking up in a small amount of toluene and crashing out with excess *n*-pentane (87%). Crystals suitable for X-ray analysis were achieved by vapor diffusion of *n*-pentane onto a CH_2Cl_2 solution of **13**. ^1H NMR (CDCl_3 , 297 K, 500 MHz): δ 0.67 (d, $J = 12.5$ Hz, 2H), δ 0.94 (d, $J = 12.5$ Hz, 2H), δ 1.26–2.37 (m, 20H), δ 4.5 (br s, 1H), δ 4.8–5.7 (br m, 3H), δ 7.27 (br s, 2H), δ 7.34 (t, $J = 7.5$ Hz, 4H), δ 7.45 (dd, $J = 7.5$, 1.5 Hz, 2H). ^{13}C NMR (CDCl_3 , 297 K, 500 MHz): δ 26.66, δ 26.98, δ 30.13, δ 30.49, δ 31.25, δ 35.81, δ 36.86, δ 37.24 (br), δ 37.52, δ 68.10 (br), δ 127.15, δ 127.28, δ 127.42, δ 127.79, δ 135.47, δ 145.78, δ 201.41. MS (ESI): m/z = (highest intensity peaks listed): 463.4 ($([\text{NHC} + \text{H}]^+)$), 663.2 ($([\text{NHC-Pd}(\text{Cl})_2 + \text{Na}]^+)$), 1303.6 ($([\text{M} + \text{Na}]^+)$), 1380.7.

4.15. *NHC-Pd(OAc)₂(OH₂)* (**14**)

Compound **13** (1 equivalent) was combined with 4.1 equivalents of AgOAc in wet CH_2Cl_2 . After stirring under ambient conditions for 1.5 h, the solution had changed from bright orange-yellow to bright yellow. The suspension was filtered over a plug of celite, and volatiles removed in vacuo, yielding **14** in quantitative yield as a yellow solid. Single crystals suitable for X-ray analysis were obtained by layering *n*-heptane onto a -20°C ethereal solution of **14**. ^1H NMR (CDCl_3 , 297 K, 300 MHz): δ 0.70–2.36 (m, 26H), δ 4.6 (broad rise in baseline, 2H, OH_2), δ 4.81 (s, 2H), δ 4.91 (s, 2H), δ 7.09 (dd, $J = 7.8$, 1.2 Hz, 2H), δ 7.32 (td, $J = 7.8$, 1.8 Hz, 2H), δ 7.38 (td, $J = 7.5$, 1.6 Hz, 2H), δ 7.49 (dd, $J = 7.5$, 1.6 Hz, 2H). ^{13}C NMR (CDCl_3 , 297 K, 300 MHz): δ 23.77, δ 26.62, δ 26.84, δ 27.73, δ 30.03, δ 30.12, δ 31.03, δ 36.83, δ 37.28, δ 37.55, δ 66.87, δ 126.09, δ 127.26, δ 127.50, δ 127.70, δ 135.83, δ 145.73, δ 181.55 (carbene carbon not detected). ESI-MS and MALDI-TOF (m/z) (highest intensity peaks listed): 627.4 ($([\text{NHC-Pd}(\text{COOCH}_3)]^+)$). Aqua ligands were not observed by ESI or MALDI-TOF.

4.16. *NHC-Pd(OCOCF₃)₂(OH₂)* (**15**)

Compound **13** (1 equivalent) was combined with 4.1 equivalents of AgOCOCF_3 in wet CH_2Cl_2 . After stirring under ambient conditions for 1.5 h, the solution had changed from bright orange-yellow to bright yellow. The suspension was filtered over a plug of celite, and volatiles removed in vacuo, yielding **15** in quantitative yield as a yellow solid. Single crystals suitable for X-ray analysis were obtained by layering *n*-heptane onto a -20°C ethereal solution of **15**. ^1H NMR (CDCl_3 , 297 K, 300 MHz): δ 0.66–2.35 (m, 26H), δ 4.85 (br s, 4H), δ 7.10 (br d, 2H), δ 7.35 (td, $J = 7.5$, 1.9 Hz, 2H), δ 7.43 (td, $J = 7.5$, 0.9 Hz, 2H), δ 7.51 (dd, $J = 7.5$, 1.8 Hz, 2H) (OH_2 protons not observed). ^{13}C NMR (CDCl_3 , 297 K, 500 MHz): δ 26.54, δ 26.77, δ 29.98, δ 30.17, δ 30.92, δ 37.06, δ 37.20, δ 37.42 (exhibits small downfield shoulder), δ 67.59, δ 115.24 (apparent quartet, though outer lines not observed, $J = 289$ Hz), δ 126.03, δ 127.77, δ 128.00, δ 128.42, δ 135.15, δ 145.41 (carbonyl and carbene carbons not observed). ESI-MS (m/z) (highest intensity peak listed): 681.4 ($([\text{NHC-Pd}(\text{COOCF}_3)]^+)$). Aqua ligands were not observed by ESI or MALDI-TOF.

4.17. Computational analysis

Density functional theory (DFT) calculations using the B3 [31]-LYP [32] functional with the 6-31G(d) basis set were employed with the GAUSSIAN 98 [33] suite of programs to perform gas phase geometry optimizations on 7^{CH_3} and $7^{\text{CH}_3\text{-TS}}$. Optimized structures were verified to be at a local minimum or a saddle point by calculation of the harmonic vibrational frequencies. “Nucleus independent chemical

shifts" (NICS) values were calculated using the GIAO-SCF method with a larger 6-311++G(d,p) basis set [27].

Acknowledgments

We appreciate financial support from the National Institutes of Health (RO1 GM67173-01) and the Dreyfus Foundation (SSS-Teacher-Scholar Award).

References

- [1] (a) W.A. Herrmann, C. Köcher, *Angew. Chem., Int. Ed. Engl.* 36 (1997) 2162; (b) A.J. Arduengo III, *Acc. Chem. Res.* 32 (1999) 913; (c) D. Bourissou, O. Guerret, F.P. Gabbaï, G. Bertrand, *Chem. Rev.* 100 (2000) 39.
- [2] (a) W.A. Herrmann, T. Weskamp, V.P.W. Böhm, *Adv. Organomet. Chem.* 48 (2001) 1; (b) W.A. Herrmann, *Angew. Chem., Int. Ed.* 41 (2002) 1290; (c) M.C. Perry, K. Burgess, *Tetrahedron: Asymm.* 14 (2003) 951.
- [3] For a leading reference to the direct use of carbenes as catalysts, see: D. Enders, T. Balensiefer, *Acc. Chem. Res.* 37 (2004) 534.
- [4] For the first example of a stable 5-membered NHC, see A.J. Arduengo III, R.L. Harlow, M. Kline, *J. Am. Chem. Soc.* 113 (1991) 361.
- [5] (a) E. Despagne-Ayoub, R.H. Grubbs, *J. Am. Chem. Soc.* 126 (2004) 10198; (b) E. Despagne-Ayoub, R.H. Grubbs, *Organometallics* 24 (2005) 338.
- [6] (a) R.W. Alder, M.E. Blake, C. Bortolotti, S. Bufali, C.P. Butts, E. Linehan, J.M. Oliva, A.G. Orpen, M.J. Quayle, *Chem. Commun.* (1999) 241; (b) F. Guillen, C.L. Winn, A. Alexakis, *Tetrahedron: Asymm.* 12 (2001) 2083; (c) P. Bazinet, G.P.A. Yap, D.S. Richeson, *J. Am. Chem. Soc.* 125 (2003) 13314.
- [7] (a) See, for example: K. Denk, P. Sirsch, W.A. Herrmann, *J. Organomet. Chem.* 649 (2002) 219; (b) V. Lavallo, J. Mafhouz, Y. Canac, B. Donnadiou, W.W. Schoeller, G. Bertrand, *J. Am. Chem. Soc.* 126 (2004) 8670; (c) Y. Canac, S. Conejero, B. Donnadiou, W.W. Schoeller, G. Bertrand, *J. Am. Chem. Soc.* 127 (2005) 7312.
- [8] (a) For comparisons of phosphines and NHCs, see: J. Huang, H.-J. Schanz, E.D. Stevens, S.P. Nolan, *Organometallics* 18 (1999) 2370; (b) M.-T. Lee, C.-H. Hu, *Organometallics* 23 (2004) 976; (c) R. Dorta, E.D. Stevens, N.M. Scott, C. Costabile, L. Cavallo, C.D. Hoff, S.P. Nolan, *J. Am. Chem. Soc.* 127 (2005) 2485.
- [9] M.M. Konnick, I.A. Guzei, S.S. Stahl, *J. Am. Chem. Soc.* 126 (2004) 10212.
- [10] (a) D.R. Jensen, M.J. Schultz, J.A. Mueller, M.S. Sigman, *Angew. Chem., Int. Ed.* 42 (2003) 3810; (b) J.A. Mueller, C.P. Goller, M.S. Sigman, *J. Am. Chem. Soc.* 126 (2004) 9724.
- [11] 2,2'-Diaminobiphenyl was synthesized quantitatively from 2,2'-dinitrobiphenyl by hydrogenation (40 psi H₂) in EtOAc, see K.M. Gillespie, C.J. Sanders, P. O'Shaughnessy, I. Westmoreland, C.P. Thickett, P. Scott, *J. Org. Chem.* 67 (2002) 3450.
- [12] For a preliminary account of this work, see: C.C. Scarborough, M.J.W. Grady, I.A. Guzei, B.A. Gandhi, E.E. Bunel, S.S. Stahl, *Angew. Chem., Int. Ed.* 44 (2005) 5269.
- [13] M.T. Reetz, H. Oka, R. Goddard, *Synthesis* (2003) 1809.
- [14] (a) S. Saba, A. Brescia, M.K. Kaloustian, *Tetrahedron Lett.* 32 (1991) 5031; (b) R.W. Alder, M.E. Blake, S. Bufali, C.P. Butts, A.G. Orpen, J. Schütz, S.J. Williams, *J. Chem. Soc., Perkin Trans. 1* (2001) 1586.
- [15] Procedure adapted from C. Drost, P.B. Hitchcock, M.F. Lappert, *J. Chem. Soc., Dalton Trans.* (1996) 3595.
- [16] Crystallographic data for the structural analyses have been deposited with the Cambridge Crystallographic Data Centre, CCDC Nos. 273345 (9^{Np}), 272584 (9^{2-Ad}), 273346 (11), 272585 (12), 272586 (13), 273348 (14), and 273347 (15). Copies of this information may be obtained free of charge from: The Director, CCDC, 12 Union Road, Cambridge, CB2 1EZ, UK, fax. (int code) +44 1223 336 033 or email: deposit@ccdc.cam.ac.uk or <http://www.ccdc.cam.ac.uk>.
- [17] W.A. Herrmann, V.P.W. Böhm, C.W.K. Gstöttmayr, M. Grosche, C.-P. Reisinger, T. Weskamp, *J. Organomet. Chem.* 617–618 (2001) 616.
- [18] (a) H.M.J. Wang, I.J.B. Lin, *Organometallics* 17 (1998) 972; (b) K.M. Lee, H.M.J. Wang, I.J.B. Lin, *J. Chem. Soc., Dalton Trans.* (2002) 2852; (c) T. Ramnial, C.D. Abernethy, M.D. Spicer, I.D. McKenzie, I.D. Gay, J.A.C. Clyburne, *Inorg. Chem.* 42 (2003) 1391; (d) W.A. Herrmann, S.K. Schneider, K. Öfele, M. Sakamoto, E. Herdtweck, *J. Organomet. Chem.* 689 (2004) 2441.
- [19] (a) Ag(I)-NHC complexes have found widespread utility as carbene transfer agents for a variety of transition metals. See the following as leading examples. Transfer to Pd: Ref. [17] and D.J. Nielsen, K.J. Cavell, B.W. Skelton, A.H. White, *Inorg. Chim. Acta* 327 (2002) 116; (b) M.C. Perry, X. Cui, K. Burgess, *Tetrahedron: Asymm.* 13 (2002) 1969; (c) V. César, S. Bellemin-Laponnaz, L.H. Gade, *Organometallics* 21 (2002) 5204; (d) J. Pytkowicz, S. Roland, P. Mangeney, G. Meyer, A. Jutand, *J. Organomet. Chem.* 678 (2003) 166; (e) R.E. Douthwaite, J. Houghton, B.M. Kariuki, *Chem. Commun.* (2004) 698; (f) B.E. Ketz, A.P. Cole, R.M. Waymouth, *Organometallics* 23 (2004) 2835; (g) S. Roland, M. Audouin, P. Mangeney, *Organometallics* 23 (2004) 3075; (h) H.M. Lee, J.Y. Zeng, C.-H. Hu, M.-T. Lee, *Inorg. Chem.* 43 (2004) 6822; (i) P.L. Chiu, C.Y. Chen, J.Y. Zeng, C.Y. Lu, H.M. Lee, *J. Organomet. Chem.* 690 (2005) 1682; Transfer to Cu: Ref. [18] and (j) P.L. Arnold, A.C. Scarisbrick, A.J. Blake, C. Wilson, *Chem. Commun.* (2001) 2340; (k) X. Hu, I. Castro-Rodriguez, K. Olsen, K. Meyer, *Organometallics* 23 (2004) 755; Transfer to Ru: (l) J.J. Van Veldhuizen, J.E. Campbell, R.E. Giudici, A.H. Hoveyda, *J. Am. Chem. Soc.* 127 (2005) 6877; (m) P.L. Chiu, H.M. Lee, *Organometallics* 24 (2005) 1692; Transfer to Rh: (n) A.R. Chianese, X. Li, M.C. Janzen, J.W. Faller, R.H. Crabtree, *Organometallics* 22 (2003) 1663; (o) E. Mas-Marzá, M. Poyatos, M. Sanaú, E. Peris, *Inorg. Chem.* 43 (2004) 2213; (p) A. Kascatan-Nebioglu, M.J. Panzner, J.C. Garrison, C.A. Tessier, W.J. Youngs, *Organometallics* 23 (2004) 1928; (q) E. Bappert, G. Helmchen, *Synlett* (2004) 1789; (r) J.A. Mata, A.R. Chianese, J.R. Miecznikowski, M. Poyatos, E. Peris, J.W. Faller, R.H. Crabtree, *Organometallics* 23 (2004) 1253; (s) A.R. Chianese, B.M. Zeglis, R.H. Crabtree, *Chem. Commun.* (2004) 2176; (t) Y.A. Wanniarachchi, M.A. Khan, L.M. Slaughter, *Organometallics* 23 (2004) 5881; (u) G. Rivera, R.H. Crabtree, *J. Mol. Catal. A: Chem.* 222 (2004) 59; (v) P.A. Evans, E.W. Baum, A.N. Fazal, M. Pink, *Chem. Commun.* (2005) 63; Transfer to Ni: (w) X. Wang, S. Liu, G.-X. Jin, *Organometallics* 23 (2004) 6002; (x) S. Winston, N. Stylianides, A.A.D. Tulloch, J.A. Wright, A.A. Danopoulos, *Polyhedron* 23 (2004) 2813; Transfer to Au: Ref. [17] and (y) S.K. Schneider, W.A. Herrmann, E. Herdtweck, *Z. Anorg. Allg. Chem.* 629 (2003) 2363;

- (z) P. de Frémont, N.M. Scott, E.D. Stevens, S.P. Nolan, *Organometallics* 24 (2005) 2411;
(aa) H.M.J. Wang, C.S. Vasam, T.Y.R. Tsai, S.-H. Chen, A.H.H. Chang, I.J.B. Lin, *Organometallics* 24 (2005) 486.
- [20] D.R. Jensen, M.S. Sigman, *Org. Lett.* 5 (2003) 63.
- [21] The NHC ligand in complex **15** was disordered in the solid state, and only the Pd and non-NHC ligands were refined anisotropically. The structure obtained defines the connectivity, but bond lengths and angles of the NHC ligand are not reliably obtained from this crystal structure and are therefore not included in Table 1.
- [22] K. Muñoz, *Adv. Synth. Catal.* 346 (2004) 1425.
- [23] M.S. Viciu, E.D. Stevens, J.L. Petersen, S.P. Nolan, *Organometallics* 23 (2004) 3752.
- [24] (a) For examples of other NHCs which form alcohol adducts, see: D. Enders, K. Breuer, G. Raabe, J. Runsink, J.H. Teles, J.-P. Melder, K. Ebel, S. Brode, *Angew. Chem., Int. Ed. Engl.* 34 (1995) 1021;
(b) M. Schöll, S. Ding, C.W. Lee, R.H. Grubbs, *Org. Lett.* 1 (1999) 953.
- [25] C.J. Kastrup, S.V. Oldfield, H.S. Rzepa, *J. Chem. Soc., Dalton Trans.* (2002) 2421.
- [26] (a) For a further description on Möbius Aromaticity, see Ref. [19] and the following: E. Heilbronner, *Tetrahedron Lett.* 5 (1964) 1923;
(b) H.E. Zimmerman, *Acc. Chem. Res.* 4 (1971) 272.
- [27] (a) For seminal references on the NICS technique, see: P.v.R. Schleyer, C. Maerker, A. Dransfeld, H.J. Jiao, N.J.R.v.E. Hommes, *J. Am. Chem. Soc.* 118 (1996) 6317;
(b) H.J. Jiao, P.v.R. Schleyer, *J. Phys. Org. Chem.* 11 (1998) 655.
- [28] (a) For references regarding the analysis of the NICS value, see: P.v.R. Schleyer, H.J. Jiao, N.J.R.v.E. Hommes, V.G. Malkin, O.L. Malkina, *J. Am. Chem. Soc.* 119 (1997) 12669;
(b) P.v.R. Schleyer, M. Manoharan, Z.X. Wang, B. Kiran, H.J. Jiao, R. Puchta, N.J.R.v.E. Hommes, *Org. Lett.* 3 (2001) 2465.
- [29] Bruker-AXS. (2000-2003) SADABS V.2.05, SAINT V.6.22, SHELXTL V.6.10 and SMART 5.622 Software Reference Manuals. Bruker-AXS, Madison, WI, USA.
- [30] P. Van Der Sluis, A.L. Spek, *Acta Crystallogr. A* 46 (1990) 194.
- [31] A.D. Becke, *J. Chem. Phys.* 98 (1993) 1372.
- [32] C. Lee, W. Yang, R.G. Parr, *Phys. Rev. B* 37 (1988) 785.
- [33] M.J. Frisch, G.W. Trucks, H.B. Schlegel, G.E. Scuseria, M.A. Robb, M.J.R. Cheeseman, V.G. Zakrzewski, J.A. Montgomery, R.E. Stratmann, J.C. Burant, S. Dapprich, J.M. Millam, A.D. Daniels, K.N. Kudin, M.C. Strain, O. Farkas, J. Tomasi, V. Barone, M. Cossi, R. Cammi, B. Mennucci, C. Pomelli, C. Adamo, S. Clifford, J. Ochterski, G.A. Petersson, P.Y. Ayala, Q. Cui, K. Morokuma, P. Salvador, J.J. Dannenberg, D.K. Malick, A.D. Rabuck, K. Raghavachari, J.B. Foresman, J. Cioslowski, J.V. Ortiz, A.G. Baboul, B.B. Stefanov, G. Liu, A. Liashenko, P. Piskorz, I. Komaromi, R. Gomperts, R.L. Martin, D.J. Fox, T. Keith, M.A. Al-Laham, C.Y. Peng, A. Nanayakkara, M. Challacombe, P.M.W. Gill, B. Johnson, W. Chen, M.W. Wong, J.L. Andres, C. Gonzalez, M. Head-Gordon, E.S. Replogle, J.A. Pople, *GAUSSIAN 98 (Revision A.10)*, Gaussian Inc., Pittsburgh, PA, 2001.